Geophysical Research Letters

RESEARCH LETTER
10.1029/2018GL077683

Key Points:
- A new model is developed for the high-frequency seismic signature of debris flows
- Seismic observations of the Montecito debris flows are used to constrain boulder sizes, flow speed, and distance
- The model applied to the Montecito debris flows suggests that early warning of up to 10 min is feasible

Supporting Information:
- Supporting Information S1

Correspondence to:
V. C. Tsai,
tsai@caltech.edu

Citation:
Lai, V. H., Tsai, V. C., Lamb, M. P., Ulizio, T. P., & Beer, A. R. (2018). The seismic signature of debris flows: Flow mechanics and early warning at Montecito, California. *Geophysical Research Letters*, *45*. https://doi.org/10.1029/2018GL077683

Received 25 FEB 2018
Accepted 19 MAY 2018
Accepted article online 30 MAY 2018

The Seismic Signature of Debris Flows: Flow Mechanics and Early Warning at Montecito, California

Voon Hui Lai[1], Victor C. Tsai[1], Michael P. Lamb[1], Thomas P. Ulizio[1], and Alexander R. Beer[1]

[1]Division of Geological and Planetary Sciences, California Institute of Technology, Pasadena, CA, USA

Abstract Debris flows are concentrated slurries of water and sediment that shape the landscape and pose a major hazard to human life and infrastructure. Seismic ground motion-based observations promise to provide new, remote constraints on debris flow physics, but the lack of data and a theoretical basis for interpreting them hinders progress. Here we present a new mechanistic physical model for the seismic ground motion of debris flows and apply this to the devastating debris flows in Montecito, California on 9 January 2018. The amplitude and frequency characteristics of the seismic data can distinguish debris flows from other seismic sources and enable the estimation of debris-flow speed, width, boulder sizes, and location. Results suggest that present instrumentation could have provided 5 min of early warning over limited areas, whereas a seismic array designed for debris flows would have provided 10 min of warning for most of the city.

Plain Language Summary Rainwater carries mud and rocks down hillsides, forming debris flows. Debris flows not only shape the landscape but also pose a major hazard to human life and infrastructure, as exemplified by what occurred in Montecito, California on 9 January 2018. An effective early warning system for debris flows would accurately determine the location and magnitude of debris flow events and could help save lives. Progress has been made in using seismic ground motions produced by debris flows for this purpose. However, the development of such early warning methods depends on effective collection of data as well as fundamental understanding of the underlying mechanics, both of which have been lacking. Here we discovered that the ground motion caused by debris flows is well recorded with current technologies and has unique characteristics that can be understood through a mechanistic model. These unique characteristics, together with the new mechanistic model, allow us to estimate key information about the debris flows, including the speed, width, rock sizes, and location. With present instrumentation, early warning could have provided 5 min of warning over limited areas. Implementation of a seismic array designed for debris flows would have provided 10 min of warning for most of the city.

1. Introduction

Debris flows are concentrated slurries of sediment and water that are typically triggered in steep mountain landscapes following intense precipitation (Iverson, 1997), and they are especially common following wildfire (Cannon, 2001; Kean et al., 2011). Debris flows are capable of rapidly transporting large volumes of sediment and large boulders over long distances, making them destructive and dangerous (Coe et al., 2014; Takahashi, 2007). Despite the significant danger and importance for landscape change (Stock & Dietrich, 2003), limited work has been done to make direct measurements of natural debris flows because they occur infrequently and are difficult and dangerous to instrument (Kean et al., 2011; Takahashi, 2007). Ground shaking measured by seismometers provides a potential breakthrough in debris flow measurements because instruments can be placed outside of the channel, and the seismic signal might be used to invert for both debris flow occurrence and debris flow mechanics (Arattano, 1999; Burtin et al., 2014; Schimmel & Hubl, 2015; Schimmel & Hubl, 2016; Turconi et al., 2015; Walter et al., 2017). However, in contrast to earthquake studies, only limited work has been done to deploy seismometers to monitor debris flows, and we lack a theoretical framework to interpret the seismic signature of debris flows to constrain flow mechanics, although important theoretical advances are being made for related phenomena in rivers and landslides (Burtin et al., 2013, 2014; Gimbert et al., 2014; Kanamori & Given, 1982; Kawakatsu, 1989; Kean et al., 2015; Tsai et al., 2012).

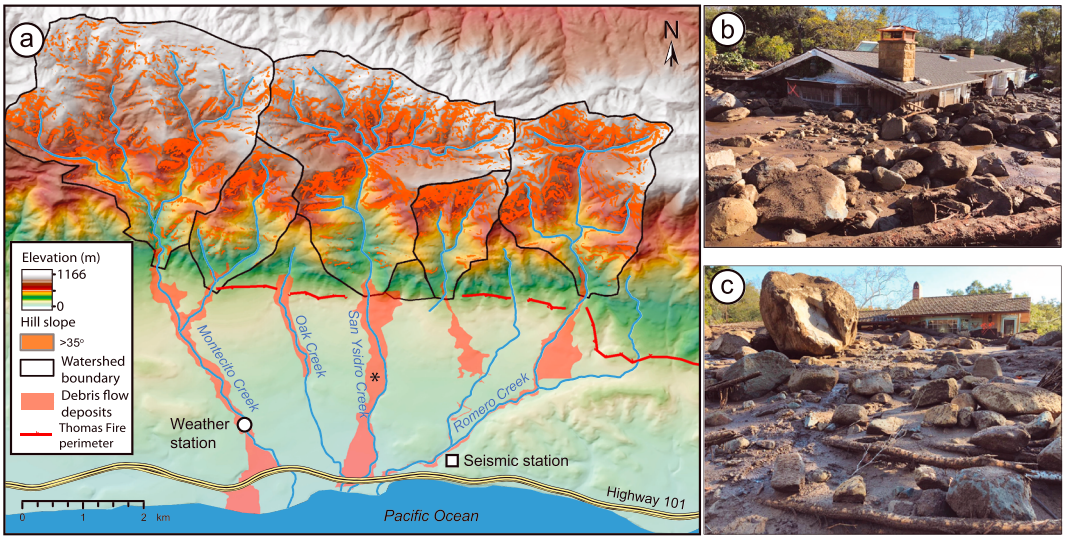

Figure 1. Montecito debris flows. (a) Map of the Montecito area showing the burned Santa Ynez Mountains to the north and the major creeks that flow through Montecito. Debris flow deposits were mapped based on aerial imagery and house damage maps produced by Santa Barbara County. Major damage was focused along Montecito and San Ysidro creeks. The seismic station is CI.QAD from the Southern California Seismic Network, and the weather station is the Montecito Station from Santa Barbara County. (b and c) Photographs following the debris flows located near the asterisk along San Ysidro Creek in (a). Photo credit: Mike Eliason, Santa Barbara County Fire.

Seismic monitoring of debris flows also has the potential to provide advanced warning of imminent debris flows that could significantly mitigate loss of life. One of the most successful advanced warning systems for debris flows in the U.S. is the joint National Oceanic and Atmospheric Administration and U.S. Geological Survey effort, which uses a combination of predicted and measured rainfall rates and past debris-flow occurrence in recently burned areas to make 24 to 48-hr predictions of the likelihood of severe debris flows (Cannon et al., 2011; NOAA-USGS Debris Flow Task Force, 2005). While these predictions are useful, by necessity, they have erred on the side of caution, with some false warnings. To complement predictions made hours to days in advance, it would be useful to have an early warning system that accurately and robustly determines debris flow characteristics in real time and hence only triggers an alert when there is a large event detected, and ideally far enough in advance that loss of life can be prevented. Applications of ground-motion based early warning systems have been slow to advance because we often lack a nearby network of permanent real-time seismic stations dedicated to debris flow detection, the seismic signature of debris flows has not been well established, and therefore early warning criteria proposed have been ad hoc and specific to each site (Schimmel & Hubl, 2016; Walter et al., 2017).

Here we address these concerns by developing a mechanistic physical model for the high-frequency ground shaking produced by debris flows and applying the model to seismic data observed within a few kilometers of the Montecito debris flows that occurred on 9 January 2018 (Figure 1a), a large event that destroyed many structures in the city of Montecito, California and caused at least 20 casualties. We demonstrate that important physical quantities can be constrained and describe implications for potential debris flow early warning application.

2. Mechanistic Model

To make a theoretical prediction for the high-frequency ($>$1 Hz) seismic ground motion produced by a debris flow, we begin with the bed load impact model of Tsai et al. (2012). A series of particles are assumed to stochastically impact a channel bed, producing seismic waves that travel to the seismic station and, to simplify the prediction, the largest amplitude ground motions are assumed to primarily come from surface waves. Additionally accounting for a minor improvement to the accuracy of the impulse response functions

(Gimbert et al., 2014), and assuming a single average source-station distance, r_0, the same model can be used to predict the ground motion due to an arbitrary set of stochastic impacts of particles, whether transported fluvially or by debris flows, yielding

$$P = \frac{0.6^2(1+\xi)^2\pi^2}{4\rho_g^2 v_c^5} \cdot m^2 \Delta w_i^2 \cdot \frac{f^3\left(\frac{f}{f_0}\right)^{5\xi}}{r_0} \cdot e^{-2\pi f r_0 (1+\xi)\left(\frac{f}{f_0}\right)^{\xi}/v_c Q} \cdot R_i. \quad (1)$$

$\xi \approx 0.25 - 0.5$ is a parameter related to how strongly seismic velocities increase with depth at the site (Tsai et al., 2012), ρ_g is the ground density, v_c is the Rayleigh-wave phase velocity at 1 Hz, m is the mass of each particle, Δw_i is the change in impact velocity at each impact, f is frequency, f_0 is a reference frequency set to 1 Hz, r_0 is the average distance of the station from the debris flow, Q is the quality factor for Rayleigh waves (assumed independent of frequency within the observed range), and R_i is the total rate of impacts (number per unit time) integrated over the entire surface, assumed to be phased randomly with respect to each other. P is the seismic power spectral density (PSD) of velocity as a function of frequency, f, and has units of $(\mathrm{m/s})^2/\mathrm{Hz}$, with absolute ground motion velocities over a frequency band Δf then given by $\sqrt{P\Delta f}$. We assume that grains are spherical and have a representative grain diameter D, discussed below, so that $m \approx \frac{\pi}{6}\rho_D D^3$, where ρ_D is the density of each grain.

In order to use equation (1) for debris flows, we must estimate Δw_i and R_i. Tsai et al. (2012) showed that seismic noise is dominated by the very coarse fraction of the load; for a nearly lognormal distribution typical of river beds, for example, D represents the 94th percentile of the grain size distribution. The coarse load of debris flows often occurs at the flow front, in a boulder snout, and these boulders are pushed from the flow behind (Takahashi, 2007). With this simple conceptualization in mind, we assume that large clasts are pushed and dragged along the riverbed in what we define as a "washboard" model, such that the average impact velocity scales with the average velocity of the flow, u. We set $\Delta w_i = 2u$ to account for significant rebound with each impact. To estimate R_i for the same washboard type model, we assume that each clast impacts the ground every time it encounters a bump in the ground surface; that is, it has an impact rate of u/L_b, where L_b is the length scale between significant bumps on the ground surface. While L_b is not well constrained, if the debris flow traverses a granular bed composed of similar material in the coarse snout, it is reasonable to assume that $L_b = D$. For debris flows over a bedrock bed, some granular flow experiments (Farin et al., 2015) suggest that when the ground is rough at many scales, clasts tend to interact most favorably with roughness elements close to the same scale, that is, that $L_b = D$ is still a reasonable assumption. Integrating over the area over which clasts are distributed, and assuming the clasts are relatively well packed results in a total $R_i = uLW/D^3$, where L is the length of the boulder-rich snout and W is the width of the flow. Making these substitutions results in

$$P = \frac{0.6^2(1+\xi)^2\pi^4\rho_D^2}{36\rho_g^2 v_c^5 r_0} \cdot LWD^3u^3 \cdot f^{3+\xi} \cdot e^{-2\pi f^{1+\xi} r_0 (1+\xi)/v_c Q}. \quad (2)$$

where f is assumed to be in Hz. (If L were much greater than r_0, one should use an effective length of $L = r_0$ in equation (2) to account for attenuation of the seismic signal.) Assuming the sediment and ground densities to be equal, substituting $\xi \approx 0.4$ (Tsai et al., 2012; Tsai & Atiganyanun, 2014), and numerically evaluating coefficients in equation (2) yields

$$P \approx 1.9 \cdot LWD^3u^3 \cdot \frac{f^{3+5\xi}}{v_c^5 r_0} e^{-\frac{8.8 f^{1+\xi} r_0}{v_c Q}}. \quad (3)$$

While this formula is only expected to provide an order-of-magnitude estimate of the seismic PSD, P, its functional form provides significant insight into the PSD signature of debris flows. Importantly, for a known set of seismic ground properties, the frequency dependence only depends on the source-station distance, r_0, and is independent of debris flow properties, whereas the amplitude of P depends strongly on both boulder size and flow speed to the third power, while having a weaker linear dependence on flow snout width and length. Interestingly, equation (3) has no direct dependence on debris flow thickness, though thickness may

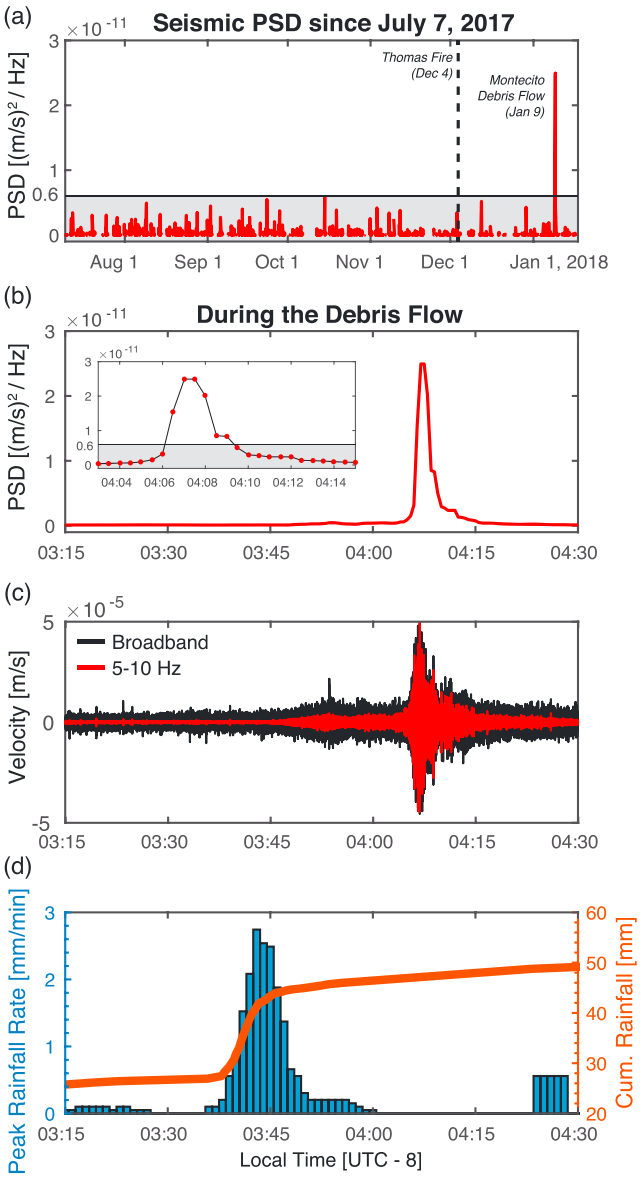

Figure 2. Detection of the Montecito debris flows from seismic ground motion data. (a) Mean power spectral density (PSD) for velocity data in a 5 to 10-Hz frequency band, averaged over 1-min time intervals, recorded on a vertical component accelerometer at seismic station CI.QAD (Figure 1a), from beginning of operation (7 July 2017) until 17 January 2018. Deglitching is necessary to remove spikes due to electrical noise (see Figures S5 and S6). PSD from the debris flow is significantly above the background noise. For early warning purposes, a threshold of 6×10^{-12} $(m/s)^2$/Hz is sufficient to distinguish the debris flow signal from other signals. (b) Mean PSD (5–10 Hz) during the debris flow episode. Inset shows the PSDs at 30-s intervals, where the signal intensifies over a short time period (<2 min.). A threshold of 6×10^{-12} $(m/s)^2$/Hz is reached by 4:06:30 a.m. (c) Seismic ground motion time series for the broadband data (in black) and filtered at 5–10 Hz (in red). The debris flow signal is dominated by the 5 to 10-Hz signal; there is also an increase in overall energy, particularly in the 1-Hz frequency range shortly after peak rainfall (see Figure 3). (d) Peak rainfall rate and cumulative rainfall recorded at the Montecito site (see Figure 1a). Peak rainfall rate is averaged over 5-min windows. Highest peak rainfall is around 3:45 a.m.

correlate with flow speed. The peak frequency f_p of equation (3) can be determined analytically by setting $dP/df = 0$ and solving for f. Doing so and solving for r_0 gives

$$r_0 = \frac{(3+5\xi)v_c Q}{2\pi(1+\xi)^2 f_p^{1+\xi}} \tag{4}$$

which can be used to estimate r_0 from measurements of f_p. The debris flow speed toward the seismometer can be calculated from changes in r_0 as a function of time recorded by the seismometer. To estimate the debris flow speed along the channel, these speeds can be corrected by an orientation factor that accounts for the direction of the flow relative to the direction to the seismometer.

Our theoretical analysis differs from previous debris flow early warning approaches and inversions for debris flow fluxes from seismic data. In previous early warning approaches (e.g., Walter et al., 2017), multiple seismic stations in a dense array were required since no mechanistic model was used to predict the absolute amplitude of seismic signal expected of a debris flow. In this work, we make a specific prediction for the absolute amplitude of the seismic signal of debris flows, allowing us to create a straightforward threshold based purely on seismic power. While previous inversions for debris flow fluxes (Kean et al., 2015) have also built upon the Tsai et al. (2012) model, this previous work has also refrained from discussing absolute amplitudes and instead has normalized seismic power relative to events with known fluxes. Since events with known fluxes are typically not available, and were not available in Montecito, this type of approach would not be feasible in most locations. Thus, while our approach of using absolute seismic amplitudes has uncertainties in the various parameters of the model, it allows for a more straightforward estimation of important physical parameters of debris flows through equations (3) and (4).

3. Data and Results

On 9 January 2018, debris flows were triggered in the Santa Ynez Mountains that border the city of Montecito to the north (Figure 1a) following a downpour of approximately 20 mm of rain over a 10-min period in Montecito at ~3:45 a.m. (Figure 2d). A month earlier, the mountains burned in one of the largest wildfires in California history, the Thomas Fire, leaving characteristic barren hillslopes and dry river channels loaded with loose sediment (DiBiase et al., 2017). Debris flows are common in southern California following wildfire, especially in steep terrain where hillslope gradients exceed the frictional stability of soil in the absence of plants (>35°); under these conditions, annual sediment yields can increase by 10-fold or more (Lamb et al., 2011). Based on local reports, debris flows began to inundate the northern parts of Montecito around 3:50 a.m. Debris flows moved through the uplands, where ~37% of the terrain exceeds 35 degrees and creek-bed gradients are ~12% (Figures 1a and S1 in the supporting information) and flowed south into a series of creeks, with gradients of ~5%, that drain south through the city of Montecito to the Pacific Ocean. Although the creeks are incised by more than 5 m into the surrounding terrain (Figure S2), the debris flows overflowed the valleys, often at bridge crossings, carrying boulders commonly 0.5–2 m, and up to 5 m, in diameter into the

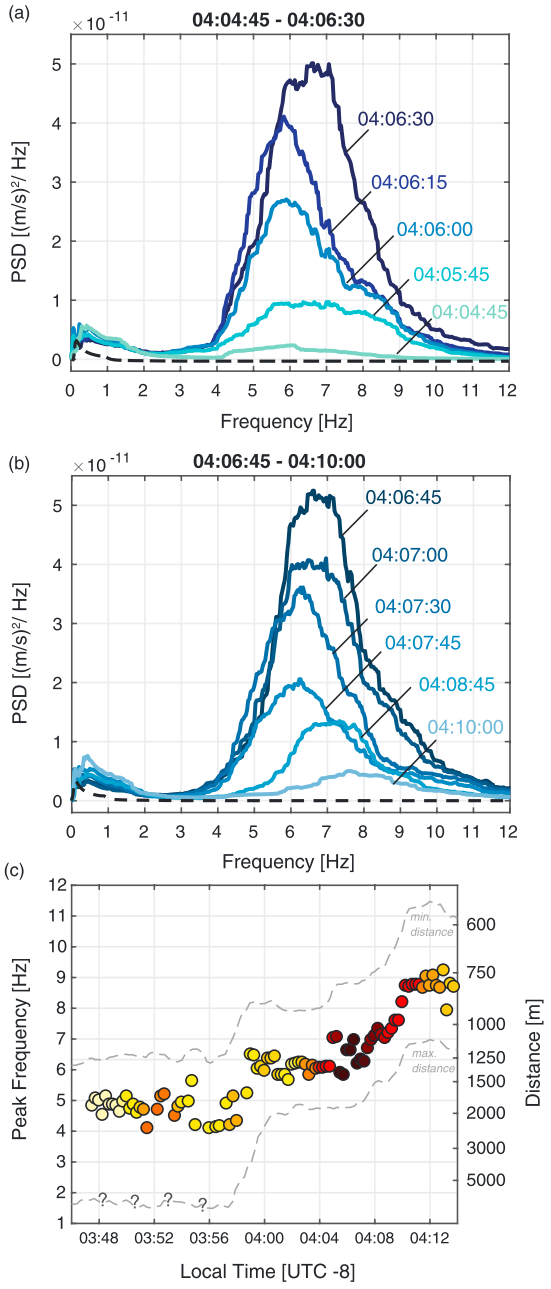

Figure 3. Evolution of power spectral density (PSD) during the debris flow. (a) PSDs recorded from 4:04:45 a.m. to 4:06:30 a.m. have initial power at 5–6 Hz (4:04:45 a.m.) over the background levels (dashed line), which increases in amplitude through 4:06:30 a.m. and changes peak frequency to 6–7 Hz. (b) PSDs recorded from 4:06:45 a.m. to 4:10:00 a.m. have power that decreases with time, with PSDs after 4:10:00 a.m. nearing background levels (dashed line). (c) Peak frequency generally increases to higher frequencies over the course of the debris flow. The warmer colors denote higher PSDs. The dashed gray lines denote the range of estimated distances after accounting for uncertainties in the seismic parameters. All PSDs are smoothed with a 2-Hz moving window. At early times, significant energy below 3 Hz from sources other than debris flows (see (a) and (b)) makes it challenging to reliably pick peak frequencies below 4 Hz. Thus, we have conservatively picked peaks that are within the more reliable 4 to 10-Hz band, despite significant energy at lower frequencies from 3:47 to 3:56 a.m. We therefore likely underestimate the distance of flows at these early times.

neighboring residential areas (Figures 1b and 1c and S3). The debris flow deposits cover ~7 km^2; damage was concentrated within a few hundred meters of the creeks and was most pronounced along Montecito and San Ysidro Creeks (Figures 1b and 1c). Hundreds of homes were damaged or destroyed and at least 20 people died.

The primary seismic station (CI.QAD) used in this analysis is located within ~250 m of Romero Creek and ~1.5 km of the zone of major damage near San Ysidro Creek (Figure 1a) and had real-time data with latencies of less than 5 s between measurement and analysis output (Stubailo et al., 2016). Ground motions at the station due to the debris flows were very anomalous, with high-frequency filtered (5–10 Hz) ground motion velocities with amplitudes in excess of 10^{-5} m/s lasting more than 10 min (Figure 2c). Despite other periods of rain, wind, ocean waves, earthquakes, and cultural noise over the 6-month deployment of the seismometer, no other time period had sustained ground motions of this magnitude when averaged over 60 s or longer (Figure 2a). The seismic signature of debris flows may be distinct; for example, shaking from earthquakes is typically shorter, and with energy distributed over a wider frequency band (Duputel et al., 2013; McNamara & Buland, 2004), strong rain, wind, water flow, and fluvial sediment transport are significantly weaker seismic sources (Burtin et al., 2008; Tanimoto & Lamontagne, 2014; Tanimoto & Valovcin, 2015), and ocean waves have lower frequency energy (Ardhuin et al., 2015; Gimbert & Tsai, 2015; Longuet-Higgins, 1950; Figure S4). Thus, a simple criterion based on time-averaged filtered ground motion amplitude exceeding 6×10^{-12} (m/s)^2/Hz accurately discriminates between the Montecito debris flows and any other event (Figure 2a). Due to significant attenuation of the seismic signal with distance from the source, this threshold was not met until 4:06:30 a.m. (Figure 2b, inset) despite reported debris flows earlier and small but significant debris flow seismic energy starting by 3:48:00 a.m. (see Figures 2c and 3c), highlighting the importance of station location for early detection as discussed below.

The success of such a simple criterion and constraints on debris flow physics can be understood in the context of equations (3) and (4). Taking estimates of seismic parameters for the site of v_c = 953 ± 200 m/s, Q = 45 ± 15, and ξ = 0.417 ± 0.05 (see supporting information; Brankman, 2009; Hauksson & Shearer, 2006; Shaw et al., 2015) allows estimates of source-station distance r_0 from observed peak frequency through equation (4). At the time of the largest ground motions at 4:06:45 a.m. in Montecito, peak frequency is observed in the range of 6–7 Hz (Figures 3a and 3b). Given the significant uncertainties in seismic parameters (Kean et al., 2015), this frequency band results in an estimated average source-station distance of 1,220 ± 600 m (see supporting information), consistent with the distance to the zones of major damage along San Ysidro and Romero Creeks (Figure 1). Because the debris flows were triggered by a brief period of intense rainfall, flows were likely active simultaneously in multiple creeks. Although the lower portion of Romero Creek is within ~250 m of the station (see Figure 1a), debris flows there appear to have been smaller and confined to the channel, consistent with the seismic data that suggest that the peak amplitude occurred farther upstream (i.e., at a distance of 1,220 ± 600 m) in Romero Creek or in

nearby San Ysidro Creek. For example, with the seismic parameters as above, a source at 250 m would have its peak at 20 Hz, far from the observed 6 to 7-Hz peak.

Due to attenuation with distance and other ambient seismic noise sources at lower frequencies, the method is not as robust for debris flows that occurred farther than ~3 km from the station, such that potential signals from Montecito Creek or the far upstream extents of San Ysidro and Romero Creeks are not reliably measured (supporting information). For example, the seismic data also show a low amplitude peak at <3 Hz and continuous for more than 4 hr, which may be due to nearby short-period ocean waves generated by the storm (Gimbert & Tsai, 2015) or water flow and standing waves (Gimbert et al., 2014; Schmandt et al., 2013) in the lower reach of Romero Creek near the seismic station. This energy overlaps significantly with signals from more distant debris flows and is the main reason that the seismic station in Santa Barbara, located ~10 km west of the Montecito station, cannot reliably be used in the analysis presented here. Nevertheless, despite being too faint to reliably separate from long-term background noise levels and thus be used for early warning purposes, both stations show clear energy above shorter-term background noise levels (e.g., Figure 2c) starting around 3:48:00 a.m. and continuing through 3:55:00 a.m. (Figure S7). These earlier, lower amplitude records are consistent with eye-witness reports of the timing of debris flows in the upper parts of Montecito and San Ysidro Creeks. Debris flows in Romero Creek, which likely occurred later due to the storm moving from west to east, or flow in the downstream section of San Ysidro Creek, are within 3 km of the Montecito seismic station but were farther away from and appear not to be detected by the Santa Barbara seismic station.

After subtracting off the <3 Hz signal, it is clear that the peak frequency from debris flows detected by the Montecito station shifts over time, from generally lower frequencies earlier (e.g., 5.5 Hz at 4:04:45 a.m. and 6.0 Hz at 4:06:00 a.m.) to higher frequencies later (e.g., 7.0 Hz at 4:08:45 a.m. and 8.0 Hz at 4:10:00 a.m.; Figures 3a and 3b), but with significant complexity in between (supporting information). Using our preferred parameters, equation (4) indicates that the shift in peak frequency corresponds to the average distance between the source and the seismometer changing from 1,540 to 1,360 m, 1,220 m, 1,100 m, and then 910 m in 1.25, 0.75, 2.0, and 1.25 min, respectively (Figure 3c). The flow path is unlikely to have been straight, and the bimodal peaks at certain times (e.g., 4:06:00 a.m., Figure 3a) suggest that at least two separate debris flow pulses were recorded. By accounting for the likely average angle between the debris flow direction and the direction of the station (~45° for lower San Ysidro Creek or ~0° for Romero Creek), we estimate an average speed over the 5.25 min of strongest signal to be $u = 2.4 \pm 1.7$ m/s. This estimate of both distance and debris flow speed can be made with a single nearby seismic station and is consistent with available information as well as observed debris flow speeds in similar terrains (Takahashi, 2007). After the seismic peak, the pattern of decreasing seismic amplitude with decreasing distance to the station suggests that the flows lost significant momentum after they were forced from the channel, spread, and deposited mud and boulders in the zones of major damage. At these late times (particularly at 4:12–4:15 a.m.), there is also a much larger fraction of seismic energy above 10 Hz (including energy at 20 Hz), in a possibly bimodal distribution, consistent with the inference of weaker but closer flows at these times (Figure S8).

Constraints on the product LWD^3u^3 can be obtained from the observed seismic amplitudes through equation (3), with a factor of ~20 uncertainties after accounting for uncertainties in the seismic parameters (see supporting information). With these uncertainties in mind, we estimate peak values of LWD^3u^3 of 8.0×10^4 m^8/s^3, with best estimates of the time history going from 7.9×10^3 m^8/s^3 at 4:04:45 a.m. to 6.8×10^4 m^8/s^3 at 4:06:00 a.m., 1.2×10^4 m^8/s^3 at 4:08:45 a.m., and 2.1×10^3 m^8/s^3 at 4:10:00 a.m. Using our estimate of $u = 2.4$ m/s and estimating $W \sim L \sim 50$ m for the width and length of the boulder snout based on channel widths ($\gtrsim$10 m; supporting information) and the lateral extent of postevent boulder fields ($\lesssim$100 m), we estimate $D = 1.3 \pm 0.6$ m at peak signal and $D = 0.7 \pm 0.4$ m closer to the station, consistent with visual observations (Figures 1b and 1c and S3). More importantly, our ability to constrain physical parameters of the debris flow provides clear guidelines for a debris flow early warning criterion based on whether LWD^3u^3 exceeds a certain threshold, where a threshold of 2,000 m^8/s^3 could correspond to a flow with $L = W = 45$ m, $D = 0.5$ m, and $u = 2$ m/s. At a nominal source-station early warning distance of 1,000 m and the seismic parameters as chosen above, a threshold of 2,000 m^8/s^3 corresponds with a maximum PSD amplitude of 6×10^{-12} $(m/s)^2/Hz$ (Figure 2a) or an average (5–10 Hz) filtered ground motion velocity threshold of 5×10^{-6} m/s. If ambient noise levels at a station were higher than the proposed corresponding threshold, our analysis implies that the straightforward early warning methodology proposed here would fail. Finally, our model suggests that the onset and decay of seismic

energy over several minutes (Figure 2b) may be characteristic of debris flows on depositional fans, with the onset being mostly due to decreasing average distance of the flow to the station, and the decay being mostly related to decreasing flow speed and grain size as the flow traverses the distal, lower gradient fan and deposits the largest boulders.

Our analysis of the ground-motion data suggests that debris flow early warning could have been accomplished for Montecito, even with a single accelerometer with moderate sensitivity in the 5 to 10-Hz frequency band providing real-time data. With the nominal threshold and estimates discussed above, the early warning time would have been approximately 5 min for locations within about 600 m of the station (supporting information). While such an early warning would not have helped for locations farther upstream, including the most heavily affected areas, a seismic network designed specifically for debris flow early warning could clearly improve upon the warning area and time. Locating multiple stations upstream of the potentially affected communities, near the border of Montecito with the Santa Ynez Mountains at each creek, could provide up to 10 min of early warning for all residents affected by the Montecito debris flows, depending on the debris flow initiation locations (supporting information). There is a trade-off between the robustness of the detection, size of the event targeted, and the amount of warning time desired, but the simple theoretical prediction of equation (3) provides a pragmatic and justifiable criterion upon which to base a warning threshold, with site-specific modifications based on the parameters discussed being clear ways in which different sites could have different ground-motion thresholds for the same targeted early warning level. While there are many practical issues that still need to be addressed before the ground-motion based debris flow early warning system proposed here would be robust and useful (e.g., Gasparini et al., 2007; Given et al., 2014; Goltz, 2002), the physics-based approach should help with better understanding the uncertainties that underlie the measurement.

4. Conclusions

We developed a mechanistic model for the high-frequency seismic signature of debris flows. The model suggests that seismic ground motion amplitudes are most sensitive to the product of four physical parameters related to the debris flow: length (L) and width (W) of the boulder snout, grain size cubed (D^3), and average speed cubed (u^3). The model also implies that peak frequency of the seismic signal depends on average distance of the debris flow from the instrument. These results have implications for what can be measured robustly with the seismic technique. For example, they suggest that the seismic observables are most sensitive to the largest clasts within the flow and are not directly sensitive to flow thickness except through the expected dependence of average speed on thickness. The results also demonstrate the need for accurate seismic parameter estimates when using the seismic technique. Applying the modeling framework to the Montecito debris flows of 9 January 2018, we find that the average distance to the nearest debris flows can be determined and that estimated grain sizes and flow speeds are consistent with observations. Our work further suggests that seismic networks designed to target debris flow early warning could provide early warning times of up to 10 min for debris flows similar to the ones that produced catastrophic results in Montecito.

Acknowledgments
The authors thank three anonymous reviewers for comments. Funding was provided by the U.S. National Science Foundation EAR-1558479 to V.C.T. and M.P.L. and EAR-1346115 to M.P.L. A.R.B. acknowledges support from the Swiss National Science Foundation. V.L. processed the seismic data, V.C.T. designed the model, M.P.L. analyzed the geomorphic data, T.P.U. measured the geographical data, and A.R.B. measured boulder data. V.C.T. and M.P.L. wrote the paper, with editorial contributions from all authors. All authors contributed to the interpretation of results. All waveform data were accessed through the Southern California Earthquake Data Center (SCEDC) at Caltech, https://doi.org/10.7909/C3WD3xH1.

References

Arattano, M. (1999). On the use of seismic detectors as monitoring and warning systems for debris flows. *Natural Hazards*, *20*(2/3), 197–213. https://doi.org/10.1023/A:1008061916445

Ardhuin, F., Gualtieri, L., & Stutzmann, E. (2015). How ocean waves rock the Earth: Two mechanisms explain microseisms with periods 3 to 300 s. *Geophysical Research Letters*, *42*, 765–772. https://doi.org/10.1002/2014GL062782

Brankman, C. (2009). Three-dimensional structure of the western Los Angeles and Ventura basins and implications for regional Earthquake hazards (Ph.D. dissertation, pp. 133). Cambridge, MA: Harvard University.

Burtin, A., Bollinger, L., Vergne, J., Cattin, R., & Nabelek, J. L. (2008). Spectral analysis of seismic noise induced by rivers: A new tool to monitor spatiotemporal changes in stream hydrodynamics. *Journal of Geophysical Research*, *113*, B05301. https://doi.org/10.1029/2007JB005034

Burtin, A., Hovius, N., McArdell, B. W., Turowski, J. M., & Vergne, J. (2014). Seismic constraints on dynamic links between geomorphic processes and routing of sediment in a steep mountain catchment. *Earth Surface Dynamics*, *2*(1), 21–33. https://doi.org/10.5194/esurf-2-21-2014

Burtin, A., Hovius, N., Milodowski, D. T., Chen, Y.-G., Wu, Y.-M., Lin, C.-W., et al. (2013). Continuous catchment-scale monitoring of geomorphic processes with a 2-D seismological array. *Journal of Geophysical Research: Earth Surface*, *118*, 1956–1974. https://doi.org/10.1002/jgrf.20137

Cannon, S. H. (2001). Debris-flow generation from recently burned watersheds. *Environmental and Engineering Geoscience*, *7*(4), 321–341. https://doi.org/10.2113/gseegeosci.7.4.321

Cannon, S. H., Boldt, E. M., Laber, J. L., Kean, J. W., & Staley, D. M. (2011). Rainfall intensity-duration thresholds for postfire debris-flow emergency-response planning. *Natural Hazards*, *59*(1), 209–236. https://doi.org/10.1007/s11069-011-9747-2

Coe, J. A., Kean, J. W., Godt, J. W., Baum, R. L., Jones, E. S., Gochis, D. J., & Anderson, G. S. (2014). New insights into debris-flow hazards from an extraordinary event in the Colorado Front Range. *GSA Today*, *24*(10), 4–10. https://doi.org/10.1130/GSATG214A.1

DiBiase, R. A., Lamb, M. P., Ganti, V., & Booth, A. M. (2017). Slope, grain size, and roughness controls on dry sediment transport and storage on steep hillslopes. *Journal of Geophysical Research: Earth Surface*, *122*, 941–960. https://doi.org/10.1002/2016JF003970

Duputel, Z., Tsai, V. C., Rivera, L., & Kanamori, H. (2013). Using centroid time-delays to characterize source durations and identify earthquakes with unique characteristics. *Earth and Planetary Science Letters*, *374*, 92–100. https://doi.org/10.1016/j.epsl.2013.05.024

Farin, M., Mangeney, A., Toussaint, R., de Rosny, J., Shapiro, N., Dewez, T., et al. (2015). Characterization of rockfalls from seismic signal: Insights from laboratory experiments. *Journal of Geophysical Research: Solid Earth*, *120*, 7102–7137. https://doi.org/10.1002/2015JB012331

Gasparini, P., Manfredi, G., & Zschau, J. (2007). *Earthquake early warning systems*. Berlin: Springer. https://doi.org/10.1007/978-3-540-72241-0

Gimbert, F., & Tsai, V. C. (2015). Predicting short-period, wind-wave generated seismic noise in coastal regions. *Earth and Planetary Science Letters*, *426*, 280–292. https://doi.org/10.1016/j.epsl.2015.06.017

Gimbert, F., Tsai, V. C., & Lamb, M. P. (2014). A physical model for seismic noise generation by turbulent flow in rivers. *Journal of Geophysical Research: Earth Surface*, *119*, 2209–2238. https://doi.org/10.1002/2014JF003201

Given, D. D., Cochran, E. S., Heaton, T., Hauksson, E., Allen, R., Hellweg, P., et al. (2014). Technical implementation plan for the ShakeAlert production system—An earthquake early warning system for the west coast of the United States (Rep. U.S. Geological Survey Open-File Rep. 2014–1097, pp. 25).

Goltz, J. D. (2002). *Introducing earthquake early warning in California: A summary of social Science and Public Policy issues* (p. 15). Sacramento California: Governor's Office of Emergency Services.

Hauksson, E., & Shearer, P. M. (2006). Attenuation models (QP and QS) in three dimensions of the southern California crust: Inferred fluid saturation at seismogenic depths. *Journal of Geophysical Research*, *111*, B05302. https://doi.org/10.1029/2005JB003947

Iverson, R. M. (1997). The physics of debris flows. *Reviews of Geophysics*, *35*, 245–296. https://doi.org/10.1029/97RG00426

Kanamori, H., & Given, J. W. (1982). Analysis of long-period seismic waves excited by the May 18, 1980, eruption of Mt. St. Helens—A terrestrial monopole? *Journal of Geophysical Research*, *87*, 5422–5432. https://doi.org/10.1029/JB087iB07p05422

Kawakatsu, H. (1989). Centroid single force inversion of seismic waves generated by landslides. *Journal of Geophysical Research*, *94*, 12,363–12,374. https://doi.org/10.1029/JB094iB09p12363

Kean, J. W., Coe, J. A., Coviello, V., Smith, J. B., McCoy, S. W., & Arattano, M. (2015). Estimating rates of debris-flow entrainment from ground vibrations. *Geophysical Research Letters*, *42*, 6365–6372. https://doi.org/10.1002/2015GL064811

Kean, J. W., Staley, D. M., & Cannon, S. H. (2011). In situ measurements of post-fire debris flows in southern California: Comparisons of the timing and magnitude of 24 debris-flow events with rainfall and soil moisture conditions. *Journal of Geophysical Research*, *116*, F04019. https://doi.org/10.1029/2011JF002005

Lamb, M. P., Scheingross, J. S., Amidon, W. H., Swanson, E., & Limaye, A. (2011). A model for fire-induced sediment yield by dry ravel in steep landscapes. *Journal of Geophysical Research*, *116*, F03006. https://doi.org/10.1029/2010JF001878

Longuet-Higgins, M. S. (1950). A theory on the origin of microseisms. *Philosophical Transactions of the Royal Society of London A*, *243*(857), 1–35. https://doi.org/10.1098/rsta.1950.0012

McNamara, D. E., & Buland, R. P. (2004). Ambient noise levels in the continental United States. *Bulletin of the Seismological Society of America*, *94*(4), 1517–1527. https://doi.org/10.1785/012003001

NOAA-USGS Debris Flow Task Force (2005). NOAA-USGS debris flow warning system—Final report (Rep. U.S. Geological Survey Circular 1283, pp. 47).

Schimmel, A., & Hubl, J. (2015). Approach for an early warning system for debris flows based on acoustic signals. In G. Lollino, et al. (Eds.), *Engineering geology for society and territory* (Vol. 3, pp. 55–58). Cham, Switzerland: Springer.

Schimmel, A., & Hubl, J. (2016). Automatic detection of debris flows and debris floods based on a combination of infrasound and seismic signals. *Landslides*, *13*(5), 1181–1196. https://doi.org/10.1007/s10346-015-0640-z

Schmandt, B., Aster, R. C., Scherler, D., Tsai, V. C., & Karlstrom, K. (2013). Multiple fluvial processes detected by riverside seismic and infrasound monitoring of a controlled flood in the Grand Canyon. *Geophysical Research Letters*, *40*, 4858–4863. https://doi.org/10.1002/grl.50953

Shaw, J. H., Plesch, A., Tape, C., Suess, M. P., Jordan, J. H., Ely, G., et al. (2015). Unified structural representation of the southern California crust and upper mantle. *Earth and Planetary Science Letters*, *415*, 1–15. https://doi.org/10.1016/j.epsl.2015.01.016

Stock, J., & Dietrich, W. E. (2003). Valley incision by debris flows: Evidence of a topographic signature. *Water Resources Research*, *39*(4), 1089. https://doi.org/10.1029/2001WR001057

Stubailo, I., Watkins, M., Devora, A., Bhadha, R. J., Hauksson, E., & Thomas, V. I. (2016). Data delivery latency improvements and first steps towards the distributed computing of the Caltech/USGS Southern California seismic network earthquake early warning system. AGU Fall General Assembly, 2016AGUFM.S23A2761S.

Takahashi, T. (2007). *Debris flow: Mechanics, prediction and countermeasures* (p. 448). London, UK: Taylor and Francis. https://doi.org/10.1201/9780203946282

Tanimoto, T., & Lamontagne, A. (2014). Temporal and spatial evolution of an on-land hurricane observed by seismic data. *Geophysical Research Letters*, *41*, 7532–7538. https://doi.org/10.1002/2014GL061934

Tanimoto, T., & Valovcin, A. (2015). Stochastic excitation of seismic waves by a hurricane. *Journal of Geophysical Research: Solid Earth*, *120*, 7713–7728. https://doi.org/10.1002/2015JB012177

Tsai, V. C., & Atiganyanun, S. (2014). Green's functions for surface waves in a generic velocity structure. *Bulletin of the Seismological Society of America*, *104*(5), 2573–2578. https://doi.org/10.1785/0120140121

Tsai, V. C., Minchew, B., Lamb, M. P., & Ampuero, J.-P. (2012). A physical model for seismic noise generation from sediment transport in rivers. *Geophysical Research Letters*, *39*, L02404. https://doi.org/10.1029/2011GL050255

Turconi, L., Coviello, V., Arattano, M., Savio, G., & Tropeano, G. (2015). Monitoring mud-flows for investigative and warning purposes: The instrumented catchment of Rio Marderello (north-western Italy). In G. Lollino, et al. (Eds.), *Engineering geology for society and territory* (Vol. 3, pp. 85–90). Cham, Switzerland: Springer.

Walter, F., Burtin, A., McArdell, B. W., Hovius, N., Weder, B., & Turowski, J. M. (2017). Testing seismic amplitude source location for fast debris-flow detection at Illgraben, Switzerland. *Natural Hazards and Earth System Sciences*, *17*(6), 939–955. https://doi.org/10.5194/nhess-17-939-2017